Peptidyl-transferase ribozymes: *trans* reactions, structural characterization and ribosomal RNA-like features

Biliang Zhang* and Thomas R Cech

Background: One of the most significant questions in understanding the origin of life concerns the order of appearance of DNA, RNA and protein during early biological evolution. If an 'RNA world' was a precursor to extant life, RNA must be able not only to catalyze RNA replication but also to direct peptide synthesis. Iterative RNA selection previously identified catalytic RNAs (ribozymes) that form amide bonds between RNA and an amino acid or between two amino acids.

Results: We characterized peptidyl-transferase reactions catalyzed by two different families of ribozymes that use substrates that mimic A site and P site tRNAs. The family II ribozyme secondary structure was modeled using chemical modification, enzymatic digestion and mutational analysis. Two regions resemble the peptidyl-transferase region of 23S ribosomal RNA in sequence and structural context; these regions are important for peptide-bond formation. A shortened form of this ribozyme was engineered to catalyze intermolecular ('*trans*') peptide-bond formation, with the two amino-acid substrates binding through an attached AMP or oligonucleotide moiety.

Conclusions: An *in vitro*-selected ribozyme can catalyze the same type of peptide-bond formation as a ribosome; the ribozyme resembles the ribosome because a very specific RNA structure is required for substrate binding and catalysis, and both amino acids are attached to nucleotides. It is intriguing that, although there are many different possible peptidyl-transferase ribozymes, the sequence and secondary structure of one is strikingly similar to the 'helical wheel' portion of 23S rRNA implicated in ribosomal peptidyl-transferase activity.

Address: Howard Hughes Medical Institute, Department of Chemistry and Biochemistry, University of Colorado, Boulder, CO 80309-0215, USA.

*Present address: Program in Molecular Medicine, University of Massachusetts Medical Center, 373 Plantation Street, Worcester, MA 01605, USA.

Correspondence: Thomas R Cech
E-mail: thomas.cech@colorado.edu

Key words: metal ions, peptidyl transferase, ribosomal RNA structure, RNA catalysis, RNA structure

Received: **3 August 1998**
Revisions requested: **18 August 1998**
Revisions received: **26 August 1998**
Accepted: **26 August 1998**

Published: **16 September 1998**

Chemistry & Biology October 1998, **5**:539–553
http://biomednet.com/elecref/1074552100500539

Introduction

Naturally occurring ribozymes efficiently catalyze the sequence-specific cleavage or ligation of RNA or DNA substrates; these natural reactions are limited to phosphate ester substrates [1]. The first demonstration that RNA can catalyze a reaction at a carbon center rather than a phosphorus center involved a modified *Tetrahymena* ribozyme that catalyzed hydrolysis of an aminoacyl ester [2]. In recent years, *in vitro* selection and *in vitro* evolution methods have provided powerful tools for isolating ribozymes that can catalyze a wide range of chemical and biochemical reactions [3–12]. Aminoacyl-transfer reactions can be catalyzed by ribozymes to form 3′-terminal aminoacyl esters and 5′-terminal esters or amide bonds [13–15]. Peptidyl-transferase reactions can also be catalyzed by ribozymes to form amide bonds between two amino acids [16].

From a chemical point of view, peptide-bond formation is the most important step in the biosynthesis of a protein. The reaction, which is accomplished in nature on the ribosome, takes place via the transfer of a peptidyl residue from peptidyl-tRNA in the ribosomal P site to the amino group of aminoacyl-tRNA in the A site (Figure 1a). Despite decades of intensive studies, the nature and the basic mechanism of the peptidyl-transferase reaction within the ribosome are still largely unknown. The discovery of catalytic RNA in the early 1980s [17,18] revitalized the hypothesis that RNA played a central role in some early stage of the evolution of life [19,20]. The 'RNA world' hypothesis proposed that RNA catalyzed its own self-replication, as well as other biochemical reactions [21–24]. The next key step occurred with the advent of RNA-catalyzed peptide synthesis. Today, ribosomal RNAs are thought to play an important role in protein biosynthesis, with the RNA having both structural and catalytic capacities [25–27].

We have demonstrated previously that peptide-bond formation can be catalyzed ~10^6-fold by RNA molecules isolated using *in vitro* selection methods [16]. The selection strategy for the peptidyl-transferase ribozymes utilized a pool of 196-mer RNA molecules randomized at 142 positions. The 5′ end of each RNA was linked by a disulfide bond to a phenylalanine residue containing a free amino group. The phenylalanine of 5′-Phe-SS-GMPS-RNA (where GMPS is guanosine-5′-monophosphorothioate) provided the nucleophilic amino group that can attack the carbonyl carbon of the methionine of AMP-Met-Bio to form a peptide bond (Figure 1b). The disulfide linkage of

Figure 1

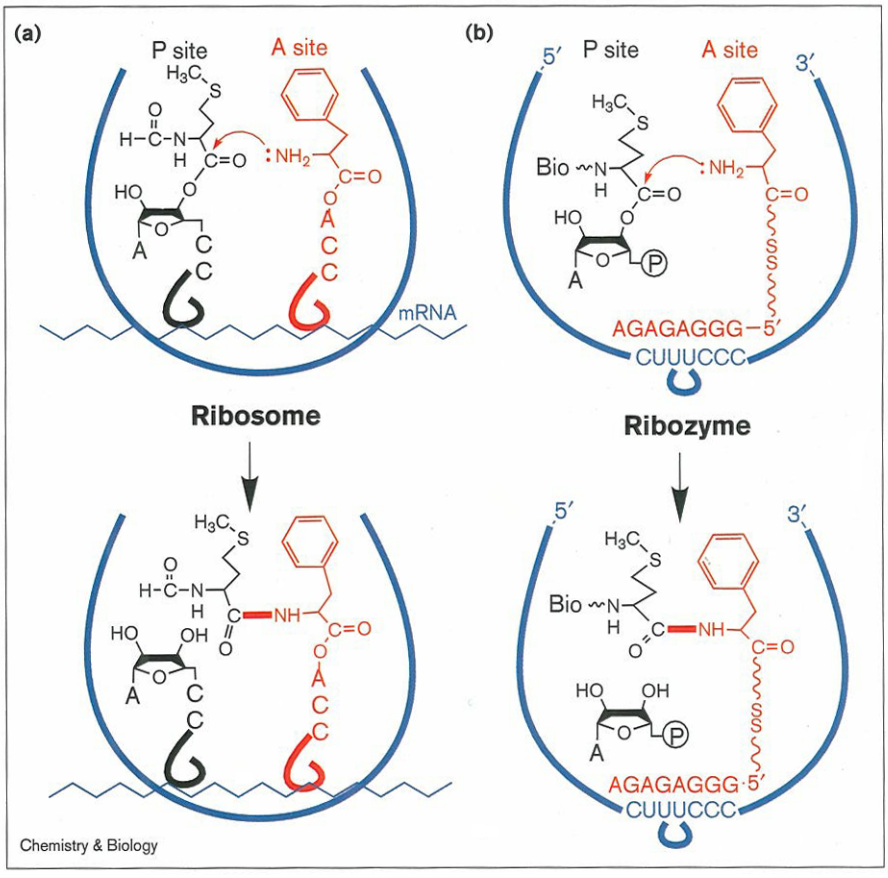

Peptide-bond formation catalyzed by ribosome and ribozyme. **(a)** The peptidyl-transferase reaction catalyzed by the ribosome involves two substrates binding at two sites: aminoacyl-tRNA at the A site and f-Met-tRNA (or peptidyl-tRNA) at the P site. **(b)** Peptide-bond formation catalyzed by the *trans* ribozyme (derived from the family II clone **25** ribozyme as described in this paper) employs two substrates: AMP-Met-Bio (black) functions as peptidyl-tRNA and 5′-Phe-linker-RNA (red) functions as aminoacyl-tRNA (wavy lines denote linker regions).

5′-Phe-SS-GMPS-RNA allowed the final dipeptide product to be cleaved from the RNA by reducing the disulfide bond with dithiothreitol (DTT) and to be characterized using high performance liquid chromatography (HPLC) mass spectroscopy.

Two major sequence families of peptidyl-transferase ribozymes were isolated previously [16]. Here, we characterize representatives from both families. We also convert a member of family II (clone **25**) into a *trans*-acting ribozyme that catalyzes peptide-bond formation in a manner even more analogous to the reaction performed by the ribosome (Figure 1).

Results

A peptidyl-transferase ribozyme has specificity for AMP

The peptidyl transferase ribozymes were selected to utilize an AMP-Met-Bio substrate [16]. The amino acid methionine is esterified to the 2′(3′) oxygen of AMP, as it is in an aminoacylated tRNA; and the amino group of methionine is blocked by derivatization with a linker that includes biotin, allowing selection on streptavidin beads. How does the peptidyl transferase ribozyme recognize its AMP-Met-Bio substrate? To test the contribution of the AMP moiety to substrate binding, we measured the ability of AMP to inhibit the clone **25** ribozyme peptidyl-transferase reaction. Figure 2a shows a typical inhibition plot of ribozyme **25** by AMP at a constant concentration (0.4 mM) of AMP-Met-Bio substrate. After measuring five apparent K_i values with appropriate concentrations of AMP-Met-Bio, a K_i of 188 μM for AMP was determined from the intercept at zero concentration of AMP-Met-Bio by a best-fit linear plot of apparent K_i versus substrate concentration. The K_i for AMP is equal to the K_m (190 μM) for the AMP-Met-Bio substrate [16], which suggests that the AMP moiety of the substrate contributes most of the binding affinity of AMP-Met-Bio for family II ribozymes.

We also studied peptidyl-transferase reactions catalyzed by the family II ribozyme using other nucleoside-5′-monophosphates as inhibitors. The time courses of peptidyl transfer in the presence of these nucleotides are shown in Figure 2b and plotted in Figure 2c. Clearly GMP, CMP, IMP and UMP do not inhibit the peptidyl-transferase reactions at 1 mM concentrations; adenosine shows intermediate inhibition; and AMP and 3′,5′-ADP are the most inhibitory. The adenosyl of the nucleotide moiety of the substrate therefore interacts specifically with the family II ribozyme, and the 5′-phosphate of the substrate appears to contribute to interactions with the ribozyme.

Figure 2

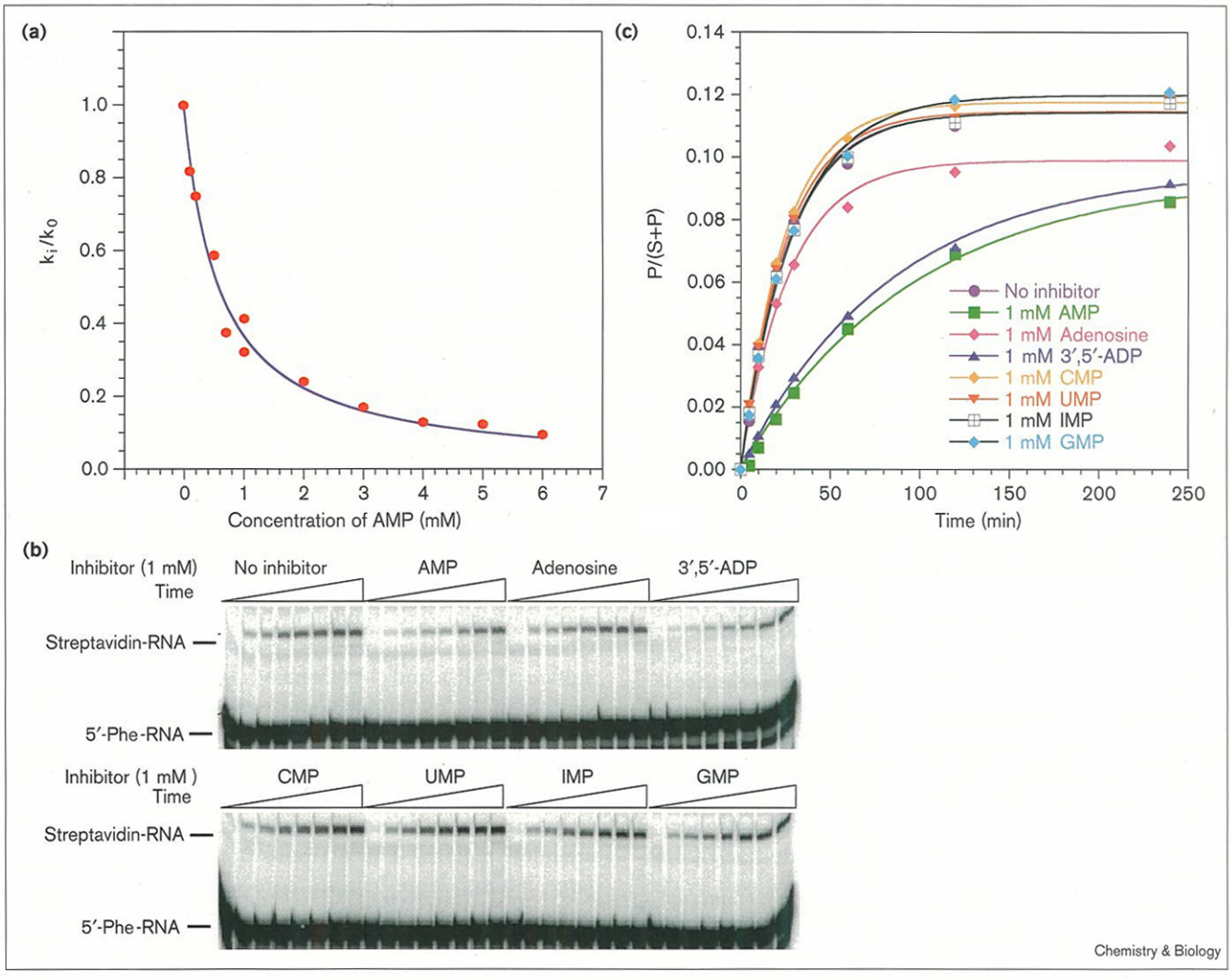

AMP binding by the clone **25** ribozyme. **(a)** AMP inhibition of peptide-bond formation catalyzed by 8 μM clone **25** ribozyme with 0.4 mM AMP-Met-Bio, 50 mM HEPES (pH 7.4) and 300 mM KCl in the presence of 100 mM $MgCl_2$ at 25°C. The best-fit apparent K_i value was obtained by fitting the data to the Morrison equation using the KaleidoGraph program. The relative observed reaction rate = $1-\{([Rbz] + [In] + K_i^{app})-[([Rbz] + [In] + K_i^{app})^2 - 4[Rbz][In]]^{1/2}\}/2[Rbz]$ with $K_i^{app} = 574$ μM. Measurement of K_i^{app} at five substrate concentrations allowed determination of $K_i = 188$ μM for AMP. **(b)** Autoradiogram of the gel-shift analysis of the time course of peptide-bond formation in the presence of nucleotide inhibitors. The time points were 0, 5, 10, 20, 30, 60, 120 and 240 min. The bottom bands are the unreacted 5′-Phe-linker-ribozyme and the top bands are the streptavidin::biotinylcaproyl-Phe-linker-ribozyme complexes. The samples were run on 7.5 M urea/8% polyacrylamide gels with 1×TBE buffer at 1000 V, 14°C. **(c)** The plots of the fraction of the product versus time in the presence of 1 mM inhibitor (data came from Figure 2b). In, inhibitor; P, product; S, substrate.

Metal-ion dependence and specificity

The peptidyl-transferase reactions of the ribozymes require metal ions [16]. We wished to know how tightly the RNA binds the metal, whether it is specific for the metal ion used during selection (Mg^{2+}) and whether different peptidyl-transferase ribozymes have similar metal ion requirements. Figure 3 shows the plots of the observed catalytic rate constants with various Mg^{2+} concentrations for clone **16** (family I) and clone **25** (family II) ribozymes. The minimum Mg^{2+} concentration required for significant catalysis by the clone **25** ribozyme was about 10 mM and maximal activity was observed at 100 mM. In contrast, the clone **16** ribozyme retained full catalytic activity at 10 mM Mg^{2+}, the lowest concentration tested. The difference in Mg^{2+} dependence between the two families is interesting because both families were selected under the same conditions (50 mM Mg^{2+}).

We next tested whether other metal ions could substitute for Mg^{2+} in the reaction. We found that Ca^{2+} could replace the Mg^{2+}, at the same concentration, for both ribozyme families, albeit giving lower activities (data not shown).

Figure 3

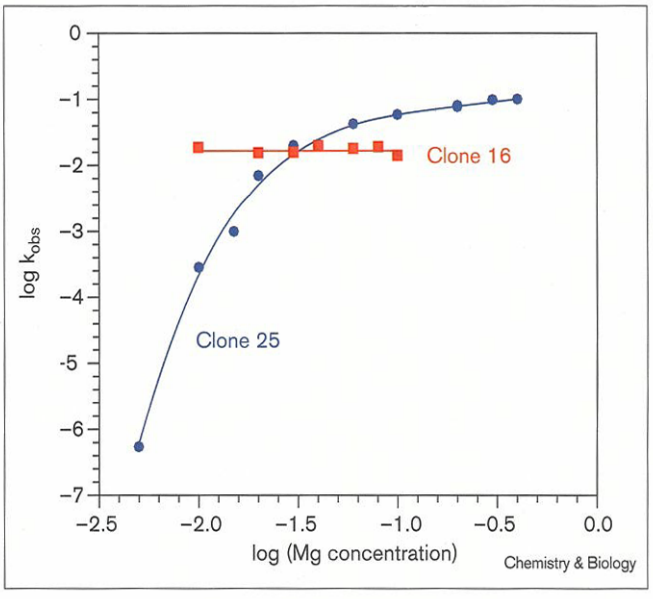

The Mg^{2+} concentration dependence of the peptidyl-transferase reactions catalyzed by the clone **16** and clone **25** ribozymes. Log plots of Mg^{2+} concentration versus the observed peptidyl-transferase reaction rates (k_{obs} in min^{-1}) are shown (clone **16** ribozyme, red; clone **25** ribozyme, blue). The reaction conditions are same as described in Figure 2, except that 800 μM AMP-Met-Bio substrate was used.

The addition of Zn^{2+} or Cu^{2+} did not increase the catalytic activity of the family II ribozyme in the presence of 20 mM Mg^{2+} and actually inhibited peptide-bond formation. Inhibition by Cu^{2+} and Zn^{2+} might be caused by deacylation of the AMP-Met-Bio substrate because Cu^{2+} and Zn^{2+} promote the cleavage of the aminoacyl-ester bonds of charged tRNAs [28].

Secondary structure of the clone 25 ribozyme

The secondary structure of the clone **25** ribozyme was initially predicted using the Mfold program [29] (Figure 4). The secondary structure model consists of eight stem helixes (P1–P8) and a large internal AU-rich loop (L3/4). Enzymatic probing was used to test this model (Figure 4). Reaction with single-strand-specific RNases T2 and U2 at A26–A31, C41–A44 and A75–A78 is consistent with the L3/4 internal loop and L4 and L5 hairpin loops. The positions of A19, A67, A99, A136, A175 and A176 in proposed bulge and hairpin regions were strongly cleaved by single-strand-specific RNase U2. The positions of G79–G80, G115 and G176 in proposed hairpin and bulge regions also showed strong cleavage by single-strand-specific nuclease S1 and RNase T1. Sites of cleavage by double-strand-specific RNase V1 located on both sides of the putative P2, P3, P5, P6 and P8 helixes provide further support that these regions are double stranded. With the exception of one region of P4 that was cleaved by single-strand-specific nucleases, the nuclease digestion results are in good agreement with the secondary-structure model of the clone **25** ribozyme.

Table 1

Deletion analysis of the clone 25 ribozyme.

	Deletion	Deletion positions	Activity
1	Wild type	NA	++
2	Internal	118–152	+
3	Internal	112–158	+
4	5′ Terminal	1–23	–
5	5′ Terminal	1–38	–
6	3′ Terminal	174–193	+/–
7	3′ Terminal	163–193	–
8	5′+3′ Terminal	1–23 and 174–193	–
9	5′+3′ Terminal	1–38 and 163–193	–

NA, not applicable. ++, full activity; +, reduced activity; +/–, low activity; –, activity not detected.

Chemical-modification analysis is also consistent with the secondary-structure model of the family II ribozyme. Chemical modification was performed with dimethyl sulfate (DMS) and 1-cyclohexyl-3-(2-morpholino-ethyl)-carbodiimide metho-p-toluene sulfonate (CMCT), and the RNA was then reverse transcribed with 5′-labeled primers resulting in chain termination at modified positions (Figure 5). The strongly modified nucleotides listed in the margins of Figure 5 are all predicted to be in single-stranded regions. These results are consistent with the large internal loop, hairpin loops and bulges of the secondary-structure model (green symbols in Figure 4).

We attempted to find the binding sites for the ribozyme substrates by footprinting. There was no change in the chemical-modification pattern of the RNA in the presence of saturating amounts of either the AMP-Met-Bio substrate or the 5′-Phe-linker (Figure 5), however. A chemical-modification footprint might not be a suitable approach for characterizing the substrate-binding sites of the clone **25** ribozyme because DMS and CMCT modification can only provide information about the interactions between the substrate and the ribozyme at Watson–Crick base-pairing positions.

Deletion analysis

We tried to minimize the size of the family II ribozyme by external and internal deletions based on the secondary structure model. The terminal deletions were from 5′-end, 3′-end, or both 5′- and 3′-ends, and internal deletions involved the P6 and P7 regions. The results of the deletion experiments are summarized in Table 1. Truncated ribozymes with internal deletions at A118–U152 and G112–C158 retained peptidyl-transferase activity, but there was a marked decrease in the catalytic rate. This

Figure 4

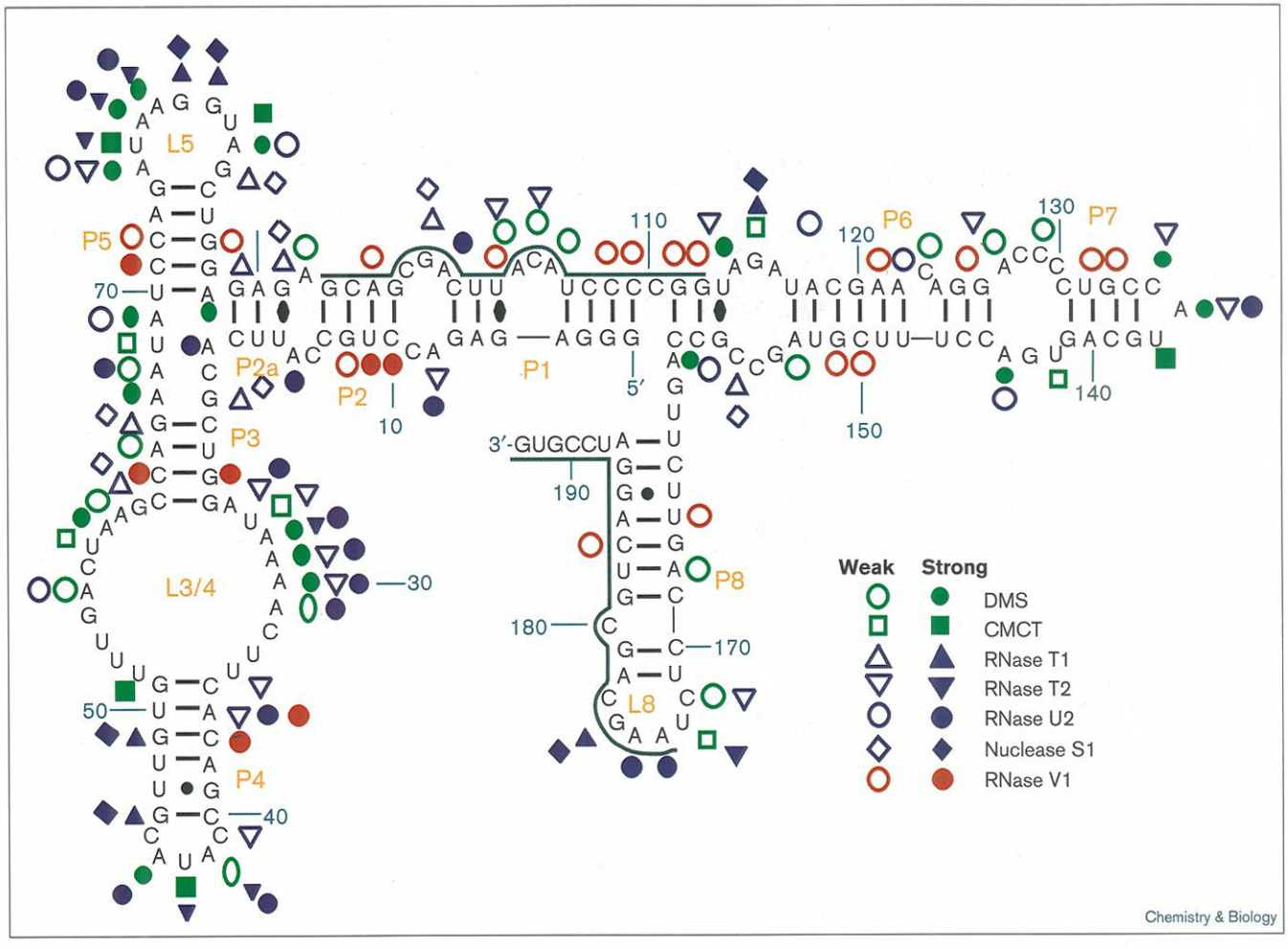

Secondary-structure model of the clone **25** ribozyme and the results of the chemical and enzymatic probing. The color symbols superimposed on the structure show positions modified by single-strand-specific CMCT or DMS (green) or cleaved by single-strand-specific nucleases (blue); the double-strand-specific probe is RNase V1 (red). The underlined nucleotides are the primer-binding sites for reverse transcription: A174–G193 is the binding site for primer 1 and G93–G112 is the binding site for primer 2.

suggests that the P6 and P7 regions might not form the catalytic center, but could be involved in tertiary interactions that stabilize the active ribozyme structure. A more dramatic decrease in catalytic activity resulted from deletion of A174–G193, and the other terminal deletions abolished catalytic activity. The fixed sequences at the 5′- and 3′-ends are therefore necessary for catalysis by the family II ribozyme and could partially comprise the active site of this class of ribozymes and/or form part of the substrate-binding sites. Further experiments are required to elucidate the precise functions of these sequences.

Trans reactions

If the catalytic entity of the RNA could be physically separated from the two substrates, investigations of structure–function relationships would be facilitated; these changes would also make the system more closely mimic the ribosome. We therefore engineered 'A-site' substrates in order to convert the clone **25** ribozyme to a trimolecular *trans*-reacting system (Figure 6). Three substrates were constructed: 20-mer, 8-mer and 4-mer oligonucleotides each with phenylalanine linked to its 5′-end (Figure 6a). Correspondingly, the 193-nucleotide (nt) clone **25** ribozyme was truncated at its 5′-end (with two 5′-guanosine nucleotides added to facilitate transcription) to generate three new ribozymes of lengths 175 nt, 187 nt, and 191 nt to be paired with the 20-mer, 8-mer, and 4-mer substrates, respectively. The third component of the trimolecular *trans* reaction was the AMP-Met-Bio substrate originally used for the *cis* reaction. The trimolecular reactions contained 8 μM of the appropriate *trans* ribozyme, 800 μM AMP-Met-Bio substrate and 20–200 μM 5′-Phe-linker-RNA substrate in the presence of 100–300 mM Mg^{2+} at 25°C. Figure 6b shows the time course of

Figure 5

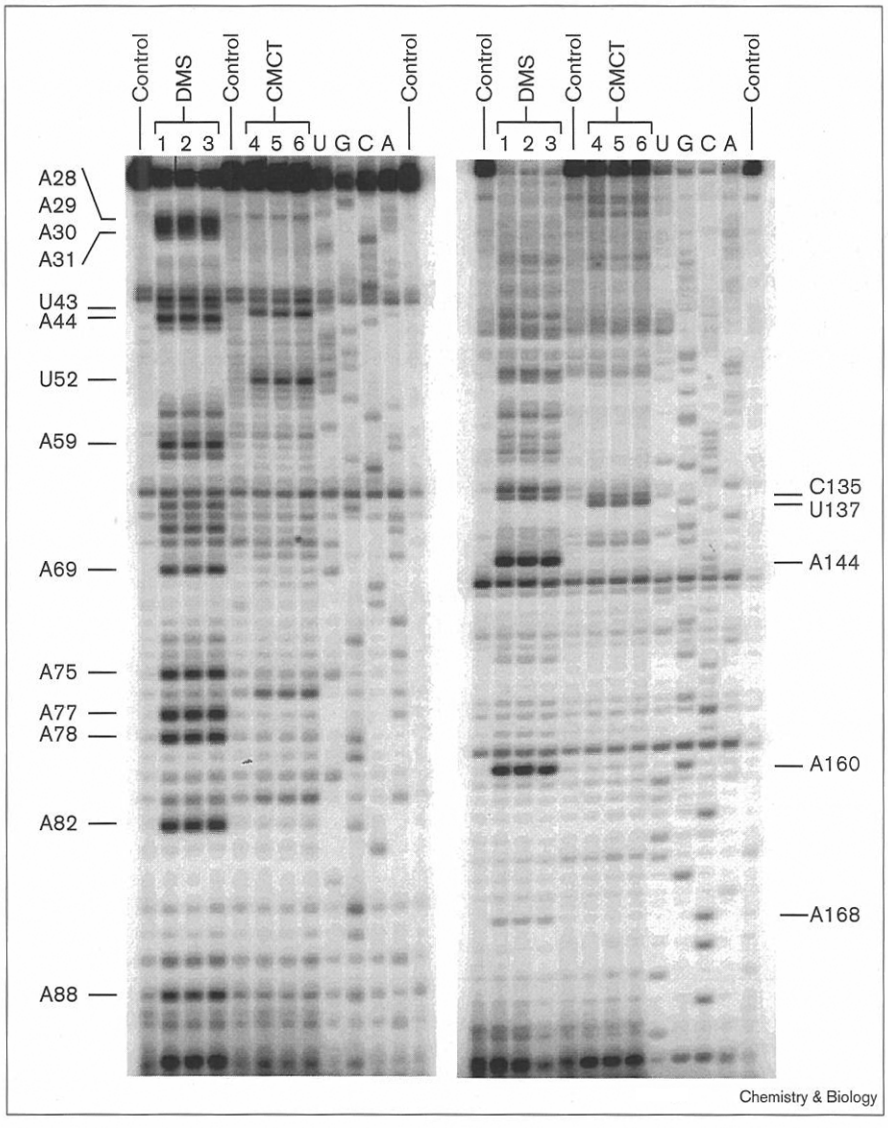

Chemical-modification probing of clone **25** ribozyme structure. Autoradiograms of a sequencing gel of clone **25** RNA (193 nt) without the Phe linker. After chemical modification with DMS and CMCT, the RNA was reverse transcribed with primer 1, which is complementary to A174–G193 (left side of figure), and with primer 2, which is complementary to G93–G112 (right side of figure); products were analyzed using gel electrophoresis and the gels scanned with a PhosphorImager. Sites of chain termination are visualized as bands preceding the modified residue by one nucleotide on polyacrylamide gel electrophoresis because modification at one of the Watson–Crick positions stops the progress of reverse transcriptase at the nucleotide preceding the modified position. Control lanes: clone **25** RNA was treated the same as other samples but the modifying agent was absent; lanes 1 and 4, clone **25** ribozyme; lanes 2 and 5, clone **25** RNA plus 1 mM 5′-Phe-linker; lanes 3 and 6, clone **25** ribozyme plus 8 mM AMP-Met-Bio.

peptide-bond formation catalyzed by the 175-nt *trans* ribozyme using 5′-Phe-20-mer RNA as the second substrate; Figure 6c shows the time course of the 187-nt *trans* ribozyme using 5′-Phe-8-mer RNA as the second substrate. The products are visualized directly as bands with retarded mobility; this assay differs from that used for the *cis* reaction, where streptavidin is added to retard the mobility of the RNA molecules that have undergone the reaction (Figure 2). DTT and streptavidin treatments were consistent with the identification of the top bands of the gels in Figure 6 as the 5′-Bio-Met-Phe-20-mer RNA and 5′-Bio-Met-Phe-8-mer RNA products (data not shown). The ribozymes can therefore carry out peptidyl transfer using two intermolecular substrates.

Both the 5′-Phe-20-mer and 5′-Phe-8-mer substrates participated in peptidyl-transferase reactions in the presence of 100 mM Mg^{2+}, but no detectable product was observed in the absence of Mg^{2+}. In contrast, the 5′-Phe-4-mer RNA substrate did not undergo a *trans* reaction in the presence of the appropriate 191-nt *trans* ribozyme with or without Mg^{2+}. The catalytic activity of the 175-mer *trans* ribozyme with the 5′-Phe 20-mer substrate was similar to the activity of the wild-type ribozyme (*cis* reaction), but decreased twofold for the 187-nt *trans* ribozyme using the 5′-Phe 8-mer RNA substrate. We also performed *trans* reactions using 2–8 μM ribozyme with 30–260 μM 8-mer substrate to quantitate product formation. We found that 1 mol of the 187-nt ribozyme can produce about 2 mol of Bio-Met–Phe-8mer product. The 187-nt ribozyme is therefore capable of at least two turnovers under these reaction conditions. A maximum of 10–20% of the clone **25** RNA is reactive in the *cis* reaction; if the *trans* reaction is equally efficient, then the

Figure 6

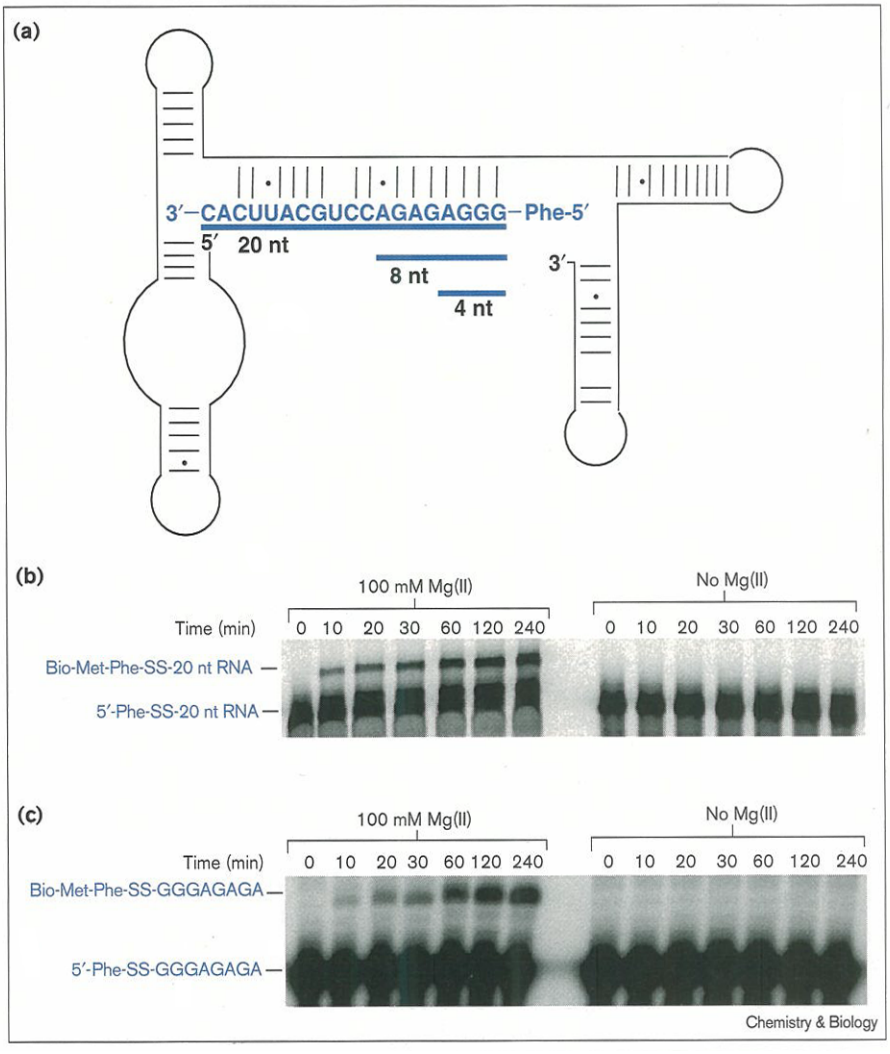

The *trans* substrate structures and the gel analysis of the bisubstrate reactions. **(a)** The line-drawing structure illustrates the clone **25** ribozyme and three new *trans* substrates: the 20-mer is shown, the 8-mer is 5′-Phe-linker-GGGAGAG and the 4-mer is 5′-Phe-linker-GGGA. The three new truncated *trans* ribozymes are 5′-GG-173 nt, 5′-GG-185 nt and 5′-GG-191 nt. **(b)** The autoradiogram of the gel analysis of *trans* reactions catalyzed by the 175-nt clone **25** *trans* ribozyme with the 5′-Phe-20-mer RNA substrate. The reactions were performed with 8 μM *trans* ribozyme and about 20 μM 5′-Phe-20-mer RNA, 800 μM AMP-Met-Bio, 300 mM KCl and 50 mM HEPES (pH 7.4) at 25°C. **(c)** Autoradiogram of the gel analysis of the *trans* reaction catalyzed by the 187-nt clone **25** *trans* ribozyme with the 5′-Phe-8-mer RNA substrate. The reactions were performed in 8 μM *trans* ribozyme, 66 μM 5′-Phe-8-mer RNA, 800 μM AMP-Met-Bio, 300 mM KCl and 50 mM HEPES (pH 7.4) at 25°C.

actual number of turnovers per active ribozyme is calculated to be 10–20.

Chemical modification by DMS and CMCT was also performed with *trans* ribozymes plus the 20-mer or 8-mer RNA substrate with or without AMP or AMP-Met-Bio (data not shown). All of these chemical-modification experiments gave the same modification patterns as shown in Figure 5, again with no indication of substrate footprints.

Testing the secondary-structure model using site-specific mutagenesis

Site-specific mutants were used to test the double-strand helices predicted by the secondary-structure model of the clone **25** ribozyme. The availability of the *trans* reaction greatly facilitated the synthesis of these mutants, because the substrate-coupling steps are not necessary for a *trans* reaction. Three helix regions (P4, P5 and P8) were mutated to change the sequence of a single side of each stem (Mut 1–6), and compensatory mutations were introduced to restore the ability of each helix to form (Figure 7a). The reactions catalyzed by the Mut 1 and Mut 2 ribozymes showed only twofold slower catalysis than that by the wild-type ribozyme (Figure 7b). The catalytic activity of the mutant ribozyme with P4 compensatory mutations (Mut 1:Mut 2) was restored to almost the level of the wild-type ribozyme. Thus, the P4 helix appears to exist, but it is not critical for catalysis. Mutation of helix P5, however, showed dramatically decreased (Mut 3) or no (Mut 4) activity. Restoration of the stem (Mut 3:Mut 4) restored activity to near wild-type levels (Figure 7b). The structure but not the sequence of helix P5 is therefore required for catalysis. Mutations of helix P8 showed an observed reaction rate for the Mut 5 ribozyme about 200 times slower than that ofthe wild-type ribozyme, whereas the Mut 6 ribozyme showed no activity. The double mutant (Mut 5:Mut 6) recovered activity relative to Mut 6, and reacted only two times slower than the wild-type ribozyme (Figure 7b). It appears that the existence of P8 and, to a lesser extent, its sequence are important for full

Figure 7

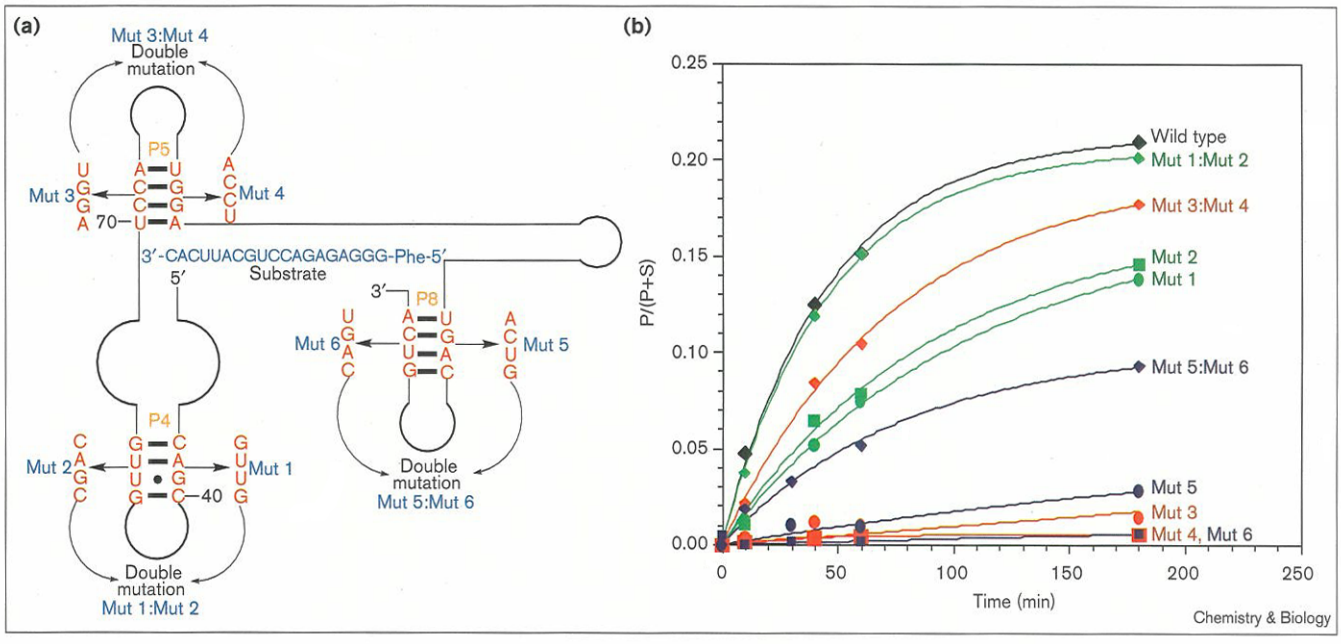

Testing the secondary-structure model of the clone **25** ribozyme. **(a)** The specific regions targeted for mutagenesis. **(b)** The time courses of the activity of the mutant ribozymes; P/(P+S), fraction product. The reactions were performed using 8 μM 175-nt *trans* ribozyme, 20 μM 5′-Phe-20-mer RNA substrate, 800 μM AMP-Met-Bio, 100 mM $MgCl_2$, 300 mM KCl and 50 mM HEPES (pH 7.4) at 25°C.

activity. These data strongly support the existence of the stems P4, P5 and P8 and attest to the importance of the P5 and P8 stems for folding and/or catalysis.

Structural similarity between the clone 25 ribozyme and the peptidyl-transferase region of 23S rRNA

Provocatively, the *in vitro* selected clone **25** ribozyme contains regions that are structurally similar to portions of the peptidyl-transferase region of domain V in 23S rRNA (Figure 8a,b). Inspection of the 23 nucleotides forming the L3/4 loop predicted from the secondary structural analysis of the ribozyme revealed that they share 70% nucleotide identity with the central loop of 23S rRNA and that they are present in the same local secondary-structure context. The top region (red) of the internal loop of clone **25** ribozyme is homologous to the top region (red) of the central loop of domain V of 23S rRNA. The bottom region (green) of the L3/4 internal loop is similar to the bottom region (green) of the peptidyl-transferase loop of 23S rRNA.

The L3/4 internal loop is essential for ribozyme catalysis. Figure 9a summarizes deletions and mutations tested. Deletion of A26–A28 (Del 26–28) resulted in a 20-fold decrease in activity, whereas deletion of A29–A31 (Del 29–31) resulted in a 150-fold decrease. Substitution of all six nucleotides (Mut 7) resulted in a 200-fold drop in activity. The peptidyl-transferase reaction was undetectable in the Mut 8 ribozyme (Figure 9a,b); considering the limit of detection of the assay, this mutant has less than 1/600 of the activity of the clone **25** ribozyme.

A second region (magenta in Figure 8) of similarity between the family II ribozymes and 23S rRNA involves six nucleotides in the L5 hairpin loop in the clone **25** ribozyme; five of these nucleotides are identical to those found in the same structural content in *E. coli* 23S rRNA (A2530–G2535), although only the AG is conserved at >90% throughout large subunit rRNAs. Testing of mutants Mut 9 and Mut 10 showed that these nucleotides in the family II ribozyme are required for its peptidyl-transferase activity (Figure 9a,c).

From the sum of these results, it seems likely that the L3/4 internal loop and L5 hairpin loop of the clone **25** ribozyme constitute at least part of the peptidyl-transferase active site of family II ribozymes. Furthermore, they lead to the testable hypothesis that these regions perform functions analogous to those performed by the corresponding sequences in the peptidyl-transferase central loop of 23S rRNA.

Discussion

The peptidyl-transferase ribozymes catalyze the transfer of an amino acid from AMP-Met-Bio to 5′-Phe-RNA to form the peptide bond of the reaction product 5′-Bio-Met–Phe-RNA. The catalytic reaction by the *trans* ribozyme described herein resembles even more closely the

Figure 8

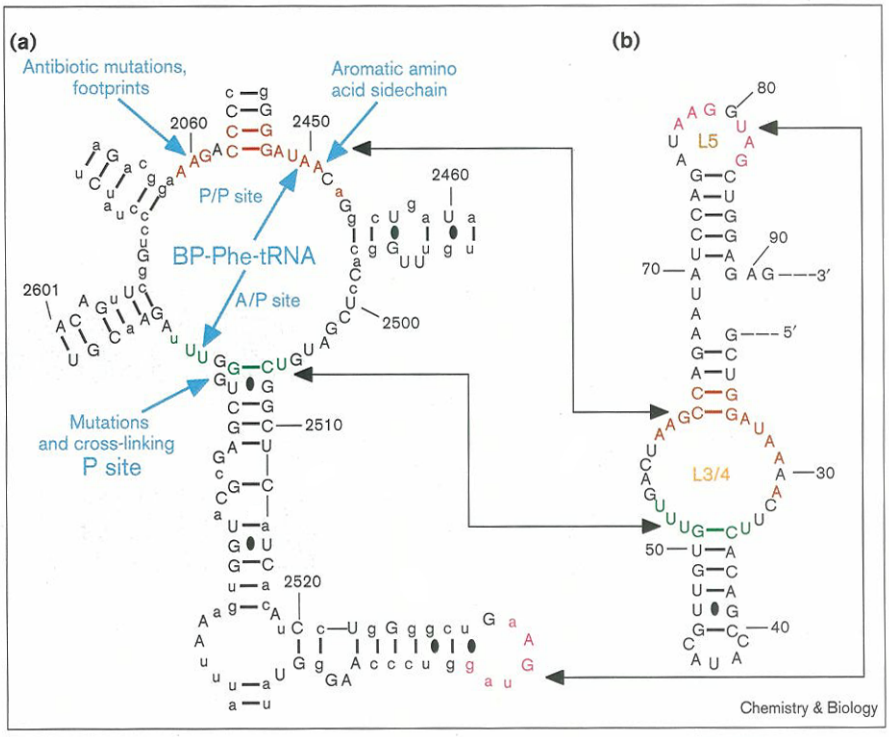

(a) The peptidyl-transferase central region of domain V of 23S rRNA, numbering according to *E. coli* 23S rRNA. The upper-case letters indicate nucleotides universally or highly conserved (> 90%) among all large subunit rRNAs. Lower-case letters indicate the less conserved nucleotides (< 90%). Arrows implicate regions involved in peptidyl-transferase activity on the basis of mutation, cross-link and footprint data. Conservation and functional data as summarized by others ([34,55]). **(b)** Partial secondary structure of the clone **25** ribozyme and 23S rRNA. Sequence identities are highlighted in red, green and magenta.

peptidyl-transferase reaction of the ribosome (Figure 1). The two amino-acid substrates of the *trans* ribozyme are each linked to a nucleotide or oligonucleotide, analogous to charged tRNAs. The *trans* ribozyme, like the ribosome, has a very specific structure required for catalysis, as evidenced by the destruction of activity by many site-specific mutations and deletions. Furthermore, the ribozyme portion of the P1 stem mimics mRNA in that it binds the oligonucleotide *trans* substrate, which mimics an anticodon; it might be possible, therefore, to program dipeptide or even oligopeptide synthesis. Mechanistic studies of peptide-bond formation catalyzed by the ribozyme might help us understand the mechanism of peptide-bond formation by the ribosome.

The *trans* reaction was calculated to convert 2 mol of 8-mer substrate to product per mole of ribozyme. A maximum of 10–20% of the clone **25** RNA is reactive in the *cis* reaction; if the same efficiency pertains to the *trans* reaction, the actual number of turnovers per active ribozyme is calculated to be 10–20. We do not know what is limiting the reaction. We assume that a better turnover number could be achieved by reengineering the *trans* ribozyme and the 5′-Phe-RNA substrate further. For comparison, Nitta *et al.* [30] reported that *in vitro*-transcribed *E. coli* 23S rRNA promoted peptide-bond formation, with 1 mol 23S rRNA producing 0.0015 mol peptide bonds. The turnover efficiency of our synthetic ribozyme is 1,300 times higher than this rRNA system.

The family II ribozymes share short regions of sequence identity with nucleotides in the central loop of domain V of 23S rRNA that are conserved among all organisms. Several lines of evidence, including RNA cross-linking, chemical footprinting, antibiotic footprinting and mutational analysis, have supported the hypothesis that this portion of 23S rRNA is the peptidyl-transferase center of the ribosome (Figure 8a) [31–35]. Chemical footprinting indicated that a number of nucleotides in domain V are located in the binding sites for the donor and acceptor tRNA substrates [36]. Cross-linking between benzophenone-derivatized peptidyl-tRNA (BP-Phe-tRNA) and A2451–C2452 of the ribosome localized this region to the peptidyl-transferase center [37]. The A2451–C2452 region is also likely to be a hydrophobic binding site where the sidechains of aromatic amino acids bind, based on substrate affinity and aromatic antibiotic inhibition experiments [38,39]. The A2059–G2061 region is also hypothesized to be the peptidyl-transferase site based on sequencing of antibiotic resistant mutants and antibiotic footprints [40,41]. Site-directed mutagenesis experiments suggested a potential A76–U2585 Hoogsteen pair between the 3′-terminal adenosine base of the peptidyl donor tRNA and the 23S rRNA [42]. Cross-linking of BP-Phe-tRNA with 23S rRNA also localized U2584 and U2585 to the ribosomal A site and A2503 and U2506 to either the A or the P site [37]. Mutational studies revealed that nucleotides Ψ2580–G2582 form a binding pocket for C75 of the peptidyl-tRNA [32].

Figure 9

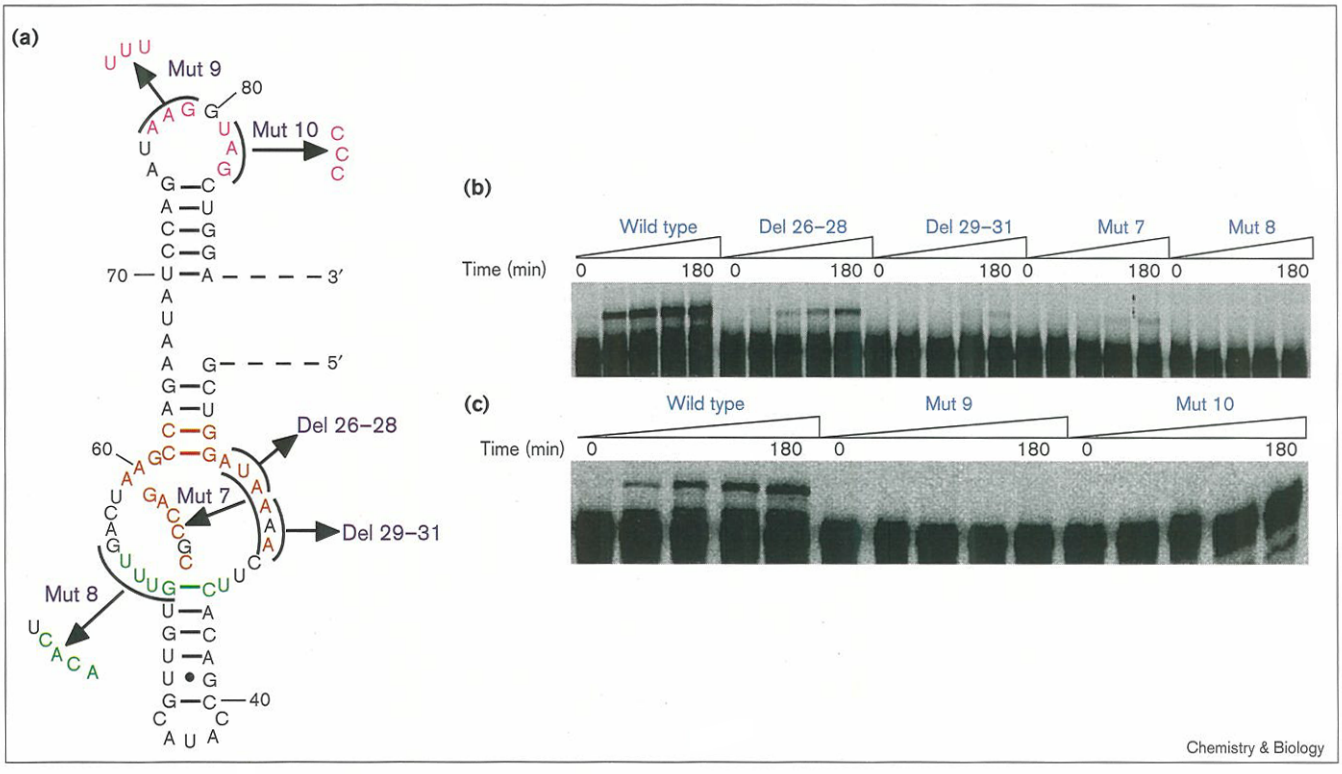

Testing the significance of the regions of similarity between clone **25** ribozyme and 23S rRNA. **(a)** The specific regions of the mutations and deletions. **(b–c)** The autoradiograms of the gel analyses of the activity of the mutant ribozymes. The reaction conditions were as described in Figure 7.

The mutational analysis presented here shows that the regions of the clone **25** ribozyme that resemble 23S rRNA are functionally important for peptidyl transfer. By analogy to 23S rRNA, these sequences might be involved in binding AMP-Met-Bio and/or the 5′-Phe-linker-RNA substrates. It is unclear whether the region (A2530–G2535) of 23S rRNA binds tRNA directly, but the similar region (L5 hairpin loop) of the clone **25** ribozyme is necessary for catalysis of peptide-bond formation. For now, our mutational data are consistent with, but do not prove, the proposal that these regions of the ribozyme perform similar functions to the peptidyl-transferase central region of 23S rRNA. Future cross-linking experiments will be needed to test this hypothesis and search for the exact substrate-binding sites.

Interestingly, the family II ribozyme (clone **25**) also shows homology to two RNA aptamer families that were selected for their ability to bind to CCdApPuro, a ribosomal peptidyl-transferase inhibitor [43]. The CCdApPuro-binding aptamers contain a consecutive eight-base binding motif matching the peptidyl-transferase loop (A2448–G2455) of 23S rRNA. The clone **25** ribozyme contains a similar region at nucleotides 26–31, providing further evidence that the large internal loop of the clone **25** ribozyme might form part of the substrate-binding sites.

Remarkably, natural selection and *in vitro* selection have yielded similar RNA structures that catalyze peptidyl transfer. The notion of 'molecular determinism' might therefore be applicable to this convergence [44]. Nevertheless, the finding of ribozyme peptidyl transferases does provide evidence for the feasibility of the RNA world hypothesis by verifying that a key assumption — protein-free RNA-mediated peptide-bond formation — is more than theoretically possible. A specific physical example can now be cited and subjected to further study.

We demonstrated that the AMP moiety is the major binding group of the AMP-Met-Bio substrate. Many small molecules including nucleotides, amino acids, dyes and organic compounds bind strongly and specifically to ribozymes and RNA aptamers. For example, the *Tetrahymena* ribozyme has a guanosine-binding site with a K_d of 500 μM [45,46]. Similarly, small ATP-binding RNA aptamers bind ATP with a K_d of about 10 μM [47]. The binding constant of arginine with another RNA aptamer is about 330 nM [48]. The binding of the AMP-Met-Bio substrate to the clone **25** ribozyme is not overwhelmingly strong (K_m = 190 μM), but it must be kept in mind that we selected for the best active ribozyme, not for the strongest-binding aptamer.

Figure 10

Synthesis of AMP-amino acid-Bio substrates **4a–d**. **(a)** N-Hydroxyl-succinimide, DCC, DMAP, DMF/DMSO, 85.8%; **(b)** L-Amino acid or N^{ε}-t-Boc-L-lysine, TEA/DMF, rt, 85-90%; **(c)** (i) Carbonyldiimidazole, DMF, 15 min; (ii) Adenosine-5′-monophosphate monosodium salt, formamide; (ii) TFA, O°C (for lysine case), 30–65%.

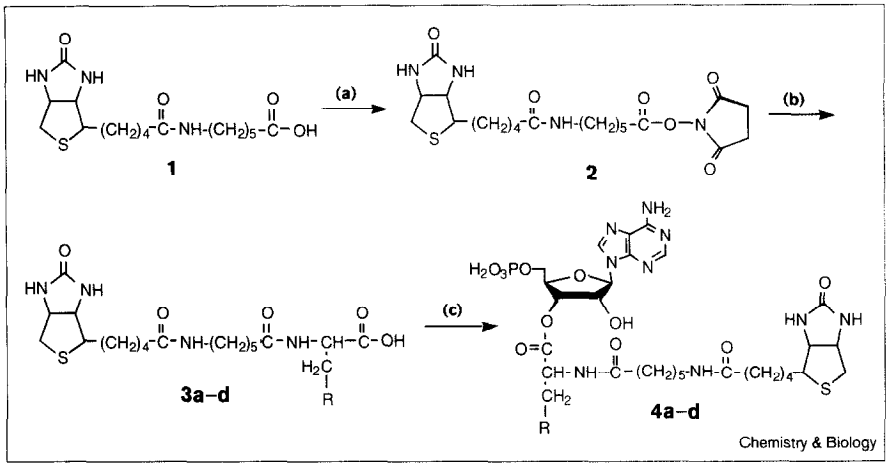

The difference in metal-ion dependence could reflect a difference in the structural folding of the two ribozyme families. In general, divalent metal ions might be required for structural stabilization of RNA, as well as catalytic activity [49–51]. Thus, the lower requirement for Mg^{2+} by family I ribozymes could reflect a more stable RNA structure. The ability of both families of ribozyme to function in Ca^{2+} is not unprecedented. It is known that the *Tetrahymena* ribozyme folds well in either Mg^{2+}, Mn^{2+} or Ca^{2+}, although Ca^{2+} by itself does not support activity [52]. In the case of the hammerhead ribozyme, Ca^{2+} can replace Mg^{2+} for activity [53]. Ribosome-catalyzed peptidyl transferase can also use Ca^{2+} in place of Mg^{2+} [54].

Significance

The order of appearance of DNA, RNA and proteins during early biological evolution has important implications for the origin of life. The 'RNA world' hypothesis, which holds that RNA was a precursor to extant life, requires that RNA be able to direct protein synthesis in addition to catalyzing RNA replication. *In vitro* selection methods were used previously to isolate ribozymes that can catalyze the transfer of a peptidyl residue from a 2′(3′)-aminoacyl-AMP substrate to an amino acid linked to the 5′-end of an RNA. Two major families from the final selection pool showed similar catalytic rates but different primary sequences and different metal ion requirements. One of these ribozymes has now been re-engineered to catalyze intermolecular peptide-bond formation using an aminoacylated nucleotide and an amino-acid-linked oligonucleotide as substrates. Our results demonstrate that a ribozyme can catalyze peptide-bond formation reactions analogous to the action of the ribosome and, most surprisingly, appears to use similar sequence and structure motifs. These findings provide evidence for the feasibility of the 'RNA world' hypothesis by demonstrating that RNA itself can make peptides, and also support the idea that ribosomal RNA has a catalytic function in the modern-day ribosome. Furthermore, the study of peptidyl transfer by the ribozymes could shed light on the mechanism of ribosomal peptidyl transfer.

Materials and methods

General and materials

^{1}H-NMR spectra were recorded on a Varian VXR 300 MHz or a Bruker AM-400 MHz spectrometer. All spectra used the residual solvent peaks as reference signals. Mass spectra were recorded on a Jeol JMS-DX-303 HF instrument (for FAB spectra) or a Hewlett-Packard 5989B HPLC-MS (for electrospray ionization mass spectra). Oligonucleotides were synthesized on an Applied Biosystems oligonucleotide synthesizer Model 394 using standard phosphoramidite chemistry. Chemicals, solvents, drying agents and inorganic salts were obtained from Fisher Scientific Co., Sigma Chemical Co., Fluka Chemical Co. or Aldrich Chemical Co. unless otherwise indicated. DMS was purchased from Aldrich and CMCT from Sigma. Anhydrous N,N-dimethyl formamide, tetrahydrofuran and methyl sulfoxide were obtained in Sure/Seal™ bottles from Aldrich Chemical Co. Guanosine-5′-monophosphorothioate (GMPS), dNTPs, NTPs, restriction enzymes and AMV reverse transcriptase were purchased from Amersham, immobilized streptavidin and streptavidin from Pierce, glycogen and Taq DNA polymerase from Boehringer Mannheim, RNase-free DNase I from Promega, α-^{32}P-ATP and γ-^{35}S-ATP from DuPont NEN. T7 RNA polymerase was supplied by A. Gooding. Aqueous buffers were prepared with autoclaved deionized water and pH values were adjusted with 1 N HCl or 1 N NaOH.

Chemical synthesis

The syntheses of aminoacyl esters **4a–d** are shown in Figure 10. The biotinylamidocaproic acid was coupled with N-hydroxysuccinimide catalyzed by DCC and then reacted with L-amino acids or N^{ε}-t-BOC-lysine to give N-biotinylamidocaproyl-L-aminoacyl (**3a–d**) in 90% yield. The compounds **3a–d** were converted to imidazole intermediates by treating with carbonyldiimidazole in DMF and esterified with adenosine-5′-monophosphate (and deprotected using trifluoroacetic acid for the lysine compound) to produce the desired aminoacyl ester products **4a–d** in 30–65% yield.

Our method for synthesis of the phenylalanine linker is outlined in Figure 11. N-t-BOC-phenylalanine-N-hydroxysuccinimide ester (**5**) was coupled with cystamine dihydrochloride salt (**6**) in triethylamin-methanol-DMF mixed solvent to give monomer **7**, which was reacted with bromoacetyl-N-hydroxysuccinimide ester and deprotected by trifluoroacetic acid to afford the final desired N-bromoacetyl-N′-phenylalaninylcystamine (**9**) in 72% yield.

Figure 11

Synthesis of the phenylalanine linker and its conjugation to the RNA. **(a)** TEA/MeOH/DMF, 24 h, rt, 58%; **(b)** Bromoacetyl-N-hydroxyl-succinimide ester, DMF, 10 h, rt; **(c)** Trifluroacetic acid, methylene chloride, 2 h, 0~5°C, 71.9%; **(d)** 5′-GMPS-RNA, 10 mM HEPES buffer, pH 7.7, overnight, 4°C.

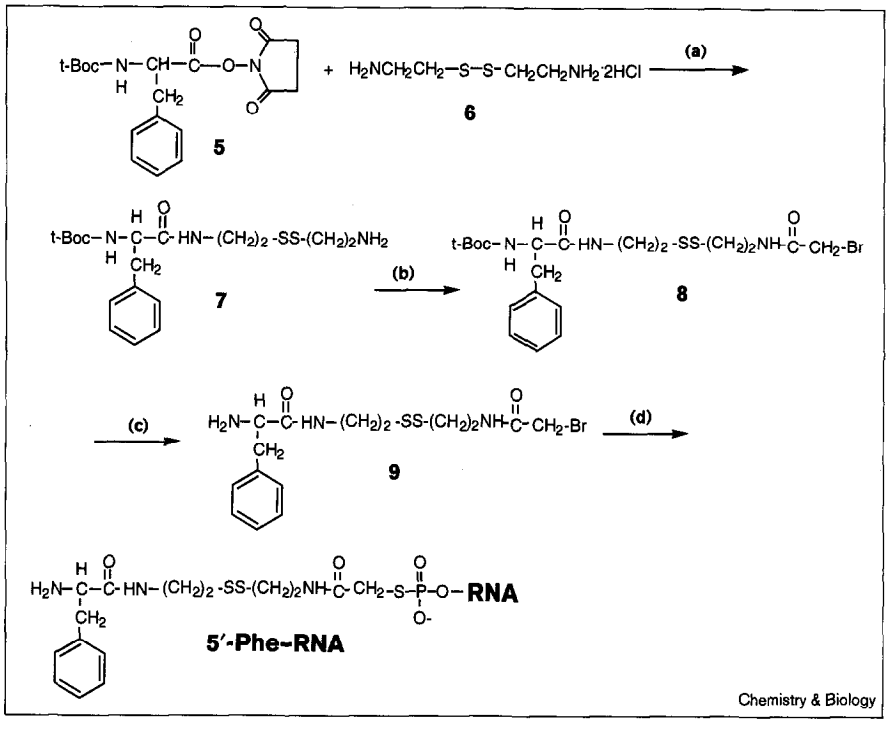

Biotinylamidocaproyl-N-hydroxysuccinimide ester **2**. Biotinyl-6-amino-caproic acid (1.0 g, 2.8 mmol), N-hydroxysuccinimide (0.33 g, 2.9 mmol) and DMAP (0.04 g, 0.31 mmol) were dissolved in 20 ml of DMSO and 20 ml of DMF. A solution of 0.64 g (3.08 mmol) of DCC in 10 ml of DMF was added to the above mixture with stirring at room temperature. The reaction solution was stirred for 24 h at room temperature, filtered and evaporated by vacuum to afford the product as a white solid that was purified by recrystallization from acetone (85.8%). ^{1}H-NMR (300 MHz, DMSO-d_6): δ 1.25-1.60 (m, 10H), 2.05 (t, 2H), 2.55 (d, 1H), 2.62 (t, 2H), 2.80 (m, 3H), 2.95 (q, 2H), 3.10 (m, 1H), 3.35 (s, 4H), 4.13 (m, 1H), 4.32 (m, 1H), 6.38 (s, NH, 1H), 6.45 (s, NH, 1H), and 7.75 (t, 1H).

N-Biotinylamidocaproyl-L-amino acid ***3a–d***. Triethylamine (1 ml) was added dropwise to a stirred solution of biotinylamidocaproyl-N-hydroxysuccinimide ester (**2**); (0.5 g, 1.1 mmol) and L-amino acid (0.25 g, 1.65 mmol) in 50 ml of DMF. The mixture was stirred for 48 h at room temperature. After removing the white precipitate by filtration, the filtrate was evaporated under reduced pressure. The organic solid was dissolved in a minimal amount of DMF and precipitated with acetone. The white solid product was collected and re-precipitated three times to give a pure product (90%).

N-Biotinylamidocaproyl-L-methionine ***3a***. ^{1}H-NMR (300 MHz, DMSO-d_6): δ1.20-1.62 (m, 16H), 1.80-2.00 (m, 2H), 2.05 (s, CH_3, 3H), 2.12 (t, 2H), 2.55 (d, 1H), 2.85 (dd, 1H), 2.95 (q, 2H), 3.10 (m, 1H), 4.12 (m, 1H), 4.30 (m, 2H), 6.38 (s, NH, 1H), 6.45 (s, 1H), 7.75 (t, NH, 1H), and 8.12 (d, NH, 1H); mass spectrum (ESI), m/e = 489(M+1).

N-Biotinylamidocaproyl-L-leucine ***3b***. ^{1}H-NMR (300 MHz, DMSO-d_6): δ0.82 (d, 3H, $C(CH_3)_2$), 0.89 (d, 3H, $C(CH_3)_2$), 1.18-1.60 (m, 15H), 2.12 (m, 4H), 2.55 (d, 1H), 2.80 (dd, 1H), 2.95 (q, 2H), 3.10 (m, 1H), 4.12 (m, 2H), 4.30 (m, 1H), 6.38 (s, NH, 1H), 6.45 (s, 1H), 7.75 (t, NH, 1H), and 8.02 (d, NH, 1H).

N-Biotinylamidocaproyl-L-phenylalanine ***3c***. ^{1}H-NMR (300 MHz, DMSO-d_6): δ1.12-1.62 (m, 14H), 2.05 (bs, 4H), 2.55 (dd, 1H), 2.85 (m, 1H), 2.95 (m, 2H), 3.10 (m, 1H), 4.12 (m, 1H), 4.25 (m, 1H), 4.40 (m, 1H), 6.38 (s, NH, 1H), 6.45 (s, 1H), 7.24 (m, 5H), 7.75 (t, NH, 1H), and 8.12 (d, NH, 1H).

N-Biotinylamidocaproyl-N$^{\varepsilon}$-t-Boc-L-lysine ***3d***. ^{1}H-NMR (300 MHz, DMSO-d_6): δ1.20-1.65 (m, 25H), 2.00-2.12 (m, 4H), 2.55 (m, 2H), 2.85 (m, 2H), 2.95 (m, 2H), 3.10 (m, 2H), 4.12 (m, 2H), 4.30 (m, 1H), 6.38 (s, NH, 1H), 6.45 (s, 1H), 6.78 (s, 1H), 7.75 (s, NH, 1H), and 8.12 (d, NH, 1H).

3′(2′)-N-Biotinylamidocaproyl-L-aminoacyl-adenosine-5′-monophosphate ***4a–d***. N-biotinylamidocaproyl-L-amino acid (0.55 g, 1.1 mmol) (**3a–d**) and 1,1′-carbonyldiimidazole (0.27 g, 1.65 mmol) in 5 ml of anhydrous DMF were stirred for 15 min at room temperature. The solution was added into a stirred solution of adenosine-5′-monophosphate monosodium (1.2 g, 3.3 mmol) in 10 ml of formamide at room temperature. The mixture was stirred overnight at room temperature and then precipitated with 200 ml of a 1:1 (v:v) mixture of acetone and ethyl ether. After centrifugation and washing with 100 ml of ethyl ether, the crude product was purified by silica gel chromatography eluted with n-butanol:acetic acid:water = 78:5:17 (v/v). The desired product was collected to give 60% yield (70% 3′-isomer and 30% 2′-isomer).

3′(2′)-N-Biotinylamidocaproyl-L-methionyl-adenosine-5′-monophosphate ***4a***. R_f = 0.55 (n-BuOH:AcOH:H_2O = 5:2:3). ^{1}H-NMR (400 MHz, D_2O): δ1.22-1.70 (m, alkyl protons), 2.12 (s, CH_3, 3H), 2.15 (m, 2H), 2.32 (m, 1H), 2.70 (d, 1H), 2.90 (d, 1H), 3.12 (m, 2H), 3.2 (m, 1H), 4.12 (m, 2H), 4.15 (m, 1H), 4.32 (m, 2H), 4.95 (m, 2′-H, 3′-isomer), 5.55 (m, 3′-H, 3′-isomer), 5.58 (m, 2′-H, 2′-isomer), 6.12 (d, 1′-H, 3′-isomer), 6.32 (d, 1′-H, 2′-isomer), 8.23 (s, 2′-isomer), 8.25 (s, 3′-isomer), 8.45 (s, 2′-isomer), and 8.50 (s, 3′-isomer); mass spectrum (ESI), m/e = 818 (M+1).

3′(2′)-N-Biotinylamidocaproyl-L-leucinyl-adenosine-5′-monophosphate ***4b***. R_f = 0.54 (n-BuOH:AcOH:H_2O = 5:2:3). ^{1}H-NMR (300 MHz, D_2O): δ0.48-0.62 (dd, 2′-isomer, $C(CH_3)_2$), 0.65-0.80 (dd, 3′-isomer, $C(CH_3)_2$), 1.12-1.58 (m, alkyl protons), 1.96 (m, 3H), 2.16 (t, 1H), 2.50 (t, 1H), 2.70 (dd, 1H), 2.90 (t, 2H), 3.02 (m, 1H), 3.85 (m, 2H), 4.22 (m, 2H), 4.30 (m, 1H), 4.35 (m, 2H), 4.95 (m, 2′-H, 3′-isomer), 5.35 (q, 3′-H, 3′-isomer),

5.39 (m, 2′-H, 2′-isomer), 5.92 (d, 1′-H, 3′-isomer), 6.08 (d, 1′-H, 2′-isomer), 8.03 (s, 3′-isomer), 8.25 (s, 2′-isomer), 8.39 (s, 2′-isomer), and 8.40 (s, 3′-isomer); mass spectrum (ESI), m/e = 800 (M+1).

3′(2′)-N-Biotinylamidocaproyl-L-phenylalanyl-adenosine-5′-monophosphate ***4c.*** $R_f = 0.53$ (n-BuOH:AcOH:H_2O = 5:2:3). ^{1}H-NMR (300 MHz, D_2O): δ0.90-1.50 (m, alkyl protons), 2.00-2.12 (m, 5H), 2.60-2.90 (m, 6H), 3.20 (m, 1H), 3.80 (m, 3H), 4.02-4.20 (m, 3H), 4.32 (m, 2H), 4.95 (m, 2′-H, 3′-isomer), 5.55 (m, 3′-H, 3′-isomer), 5.58 (m, 2′-H, 2′-isomer), 6.12 (d, 1′-H, 3′-isomer), 6.32 (d, 1′-H, 2′-isomer), 6.80 (m, 2′-isomer), 7.10 (m, 3′-isomer), 8.00 (dd, 1H), 8.35 (s, 2′-isomer), and 8.40 (s, 3′-isomer); mass spectrum (ESI), m/e = 834 (M+1).

3′(2′)-N-Biotinylamidocaproyl-L-lysinyl-adenosine-5′-monophosphate ***4d.*** $R_f = 0.48$ (n-BuOH:AcOH:H_2O = 5:2:3). ^{1}H-NMR (300 MHz, D_2O): δ1.22-170 (m, alkyl protons), 2.08 (m, 2H), 2.20 (m, 1H), 2.60 (d, 1H), 2.80 (m, 2H), 2.95 (m, 1H), 3.12 (m, 1H), 3.95 (m, 2H), 4.22 (m, 1H), 4.38 (m, 2H), 4.85 (m, 2′-H, 3′-isomer), 5.40 (m, 3′-H, 3′-isomer), 5.50 (m, 2′-H, 2′-isomer), 6.08 (d, 1′-H, 3′-isomer), 6.20 (d, 1′-H, 2′-isomer), 8.30 (s, 3′-isomer), 8.48 (s, 2′-isomer), 8.50 (s, 2′-isomer), and 8.52 (s, 3′-isomer); mass spectrum (ESI), m/e = 815 (M+1).

N-t-BOC-L-Phenylalanyl-cystamine ***7.*** To a solution of cystamine (6.8 g, 30 mmol) and 20 ml of triethylamine in 100 ml of methanol was added a solution of t-BOC-L-phenylalanyl-N-hydroxysuccinimide ester (3.62 g, 10 mmol) in 40 ml of DMF at room temperature. The mixture was stirred overnight at room temperature. After removing the solvent by distillation under reduced pressure, the residue was dissolved in ethyl acetate and washed with saturated sodium bicarbonate once and with water twice. The organic layer was dried with anhydrous sodium sulfate and evaporated by rotavapor. The crude product was purified by flash chromatography with silica gel (eluted with 10% methanol in methylene chloride) to give the pure desired product (58%). ^{1}H-NMR (300 MHz, $CDCl_3$): δ 1.25 (s, 9H), 2.65-2.79 (m, 4H), 2.92 (dd, 2H), 3.23-3.41 (m, 2H), 4.15 (m, 1H), 6.92 (d, NH, 1H), 7.25 (m, aromatic, 5H) and 8.15 (t, NH, 1H); mass spectrum (ESI), m/e = 400 (M+1).

Bromoacetyl-N-hydroxysuccinimide ester. A solution of DCC (11.35 g, 55 mmol) in 30 ml of anhydrous THF was added to a solution of N-hydroxysuccinimide (5.75 g, 50 mmol), bromoacetic acid (6.94 g, 50 mmol) and DMAP (0.61 g, 5 mmol) in 80 ml of anhydrous THF at 0°C (ice-bath). The mixture was stirred overnight at room temperature. After filtering out the precipitate, the filtrate was evaporated under reduced pressure to dryness. The crude product was purified by recrystallization from hot ethyl acetate (92%). ^{1}H-NMR (300 MHz, $CDCl_3$): δ 2.82 (s, 4H) and 4.05 (s, $BrCH_2$, 2H).

N-L-Phenylalanyl-N′-bromoacetyl-cystamine **9**. A solution of N-t-BOC-L-phenylalanylcystamine (**7**) (1 g, 2.5 mmol) and bromoacetyl N-hydroxysuccinimide ester (1 g, 4.2 mmol) in 30 ml of anhydrous DMF was stirred for 10 h at room temperature. After removing the solvent by evaporation under reduced pressure, the residue was dissolved in chloroform and any insoluble material was removed by filtration. The clear solution was loaded on a silica gel column and first eluted with chloroform and then eluted with 10% methanol in chloroform to collect the pure desired product. The product **8** was dissolved in 20 ml of methylene chloride and deprotected with 2 ml of trifluoroacetic acid at 0–5°C (ice-water bath). The mixture was stirred for 2 h at 0–5°C, and then warmed up to room temperature for 10 min. After evaporating the solvent under reduced pressure, the solid compound was triturated three times with ethyl ether to give the pure product **9** (71.9%). ^{1}H-NMR (300 MHz, DMSO-d_6): δ 2.51-2.78 (m, 6H), 2.98 (m, 2H), 3.35 (m, 2H), 3.85 (s, 2H), 3.95 (t, 1H), 7.20-7.35 (m, 5H), 8.20 (wide, NH_2, 2H), 8.50 (t, 1H) and 8.59 (t, 1H); mass spectrum (ESI), two equal intensity mass peaks: m/e = 420 (M+1) [^{35}Br] and 422(M+3) [^{37}Br].

Ribozyme synthesis

All *trans* ribozymes were prepared by runoff transcription with T7 RNA polymerase using the products of PCR amplification of the corresponding cDNAs as templates. Transcription reactions were carried out in the presence of 12 mM Mg^{2+}, 2 mM each GTP, ATP, CTP and UTP, and 10 μg of DNA template in a total 200 μl solution. For *cis* reactions, the ribozymes were synthesized by runoff transcription in the presence of guanosine-5′-monophosphorothioate (GMPS) with a ratio of GMPS:GTP:ATP:CTP:UTP = 8:0.4:1:1:1 mM and [α-^{32}P]-ATP. The body-labeled 5′-GMPS-ribozymes were purified by denaturing 7.5 M urea/8% polyacrylamide gel electrophoresis and reacted with Phe-linker-CH_2Br in 10 mM HEPES (pH 7.7) and 1 mM EDTA at 4°C overnight. The 5′-Phe-linker-ribozymes were similarly purified by denaturing polyacrylamide gel electrophoresis, resuspended in pure water and stored in −70°C freezer.

5′-Phe-linker-RNA substrate preparation

5′-Phe-linker-GGGAGAGA-3′, 5′-Phe-linker-GGGAGAGACCUGCCA-UUCA-3′ and 5′-Phe-linker-GGGA-3′. RNA substrates were prepared in the same manner as the 5′-Phe-linker-ribozymes described above. Alternatively, RNA oligonucleotides were synthesized on an automated synthesizer and reacted with [γ-^{35}S]-ATP catalyzed by T4 polynucleotide kinase. The 5′-[^{35}S]-GMPS-RNAs were purified by denaturing 20% polyacrylamide gel electrophoresis and then treated with Phe-linker-CH_2Br to afford the 5′-Phe-linker-RNA used for the *trans* reactions.

Kinetic assays

All single turnover *cis* reactions were carried out with uniformly [α-^{32}P]-ATP-labeled ribozyme and excess AMP-Met-Bio substrate (≥ 100-fold) in 50 mM HEPES (pH 7.4), 300 mM KCl and 50 mM $MgCl_2$ at 25°C. The RNA was preincubated with buffer and Mg^{2+} for 10 min at 50°C, and cooled to room temperature (~20 min). The reaction was initiated by addition of AMP-Met-Bio substrate. Aliquots of 2 μl were removed from 20 μl reaction mixtures at specific time points, quenched with an equal volume of stop buffer containing 100 mM HEPES (pH 7.4) and 100 mM EDTA and frozen on dry ice. Thawed samples were incubated with 10 μg of streptavidin in the binding buffer (20 mM HEPES, pH 7.4, 5.0 mM EDTA and 1.0 M NaCl) at room temperature for 20 min prior to mixing with 0.25 volumes of formamide loading buffer (90% formamide, 0.01% bromophenol blue and 0.025% xylene cyanol). The biotinylated RNA products were resolved by electrophoresis on 7.5 M urea/8% polyacrylamide gels. The fraction of product formation relative to total substrate and product at each time point was quantitated using a Molecular Dynamics PhosphorImager.

Trans *reaction assays*

The *trans* reactions were performed in a similar fashion as described above, except that ribozymes were preincubated with 5′-Phe-linker-RNA substrate and streptavidin was not added because it was not needed to resolve the reaction products from the unreacted RNAs. The ribozyme was preincubated in the presence of Mg^{2+} with at least a 10-fold greater concentration of 5′-Phe-linker-RNA substrate for 10 min at 50°C, then cooled slowly to room temperature for about 20 min. Then 2 μl of 8 mM AMP-Met-Bio (10 ×) solution was added to initiate the reaction at 25°C. A 2 μl sample was removed from the 20 μl reaction mixture at each specific time point, quenched with an equal volume of formamide loading buffer (90% formamide, 0.01% bromophenol blue and 0.025% xylene cyanol) and by immediately freezing on dry ice. The samples were loaded on a denaturing 20% polyacrylamide gel. The rest of the analysis was as described above.

Chemical modification

A total of 30 μl of 193-nt clone 25 RNA (24 pmol) or 175-nt clone **25** RNA (30 pmol) with 20 nt RNA substrate (30 pmol) solution was annealed in the reaction buffer (10 × DMS buffer: 500 mM HEPES, pH 7.4; 3.0 M KCl; 10 × CMCT buffer: 500 mM $NaB(OH)_3$, pH 8.0; 3.0 M KCl) by boiling for 90 s at 90°C, and air-cooling to room temperature for about 10 min. Then 3 μl of 1.0 M $MgCl_2$ and/(when indicated) 3 μl of 8 mM AMP-Met-Bio (or 40 mM AMP and 1 mM Phe-linker-CH_2Br or 30 μM 5′-Phe-linker-RNA) was/were added. The mixture was incubated for 10 min at 50°C, cooled to room temperature for 20 min.

Fresh DMS stock solution (3 µl, 1:10 = DMS:ethanol) or fresh CMCT stock solution (5 µl, 42 mg/l CMCT in water) was added and incubated for 20 min (DMS) or 30 min (CMCT) at 25°C. The reaction was stopped by addition of 15 µl of stop solution (1.5 M NaOAc [pH 5.5], 1.0 mM EDTA and 0.1 µg/µl linear acrylamide) and precipitated with 450 µl of cold ethanol (20–30 min on dry ice and centrifuged for 10–15 min). The pellet was resuspended in 20 µl of water.

Reverse transcription

Primer 1: 5′-CACGGATCCTGACGCTGCTT-3′, corresponding to residues 193–174 of clone **25** ribozyme; primer 2: 5′-CCGGGGATG-TAAGGTCGCTGC-3′, corresponding to residues 112–93 of clone **25** ribozyme. 1 µl of 5′ labeled primer (2×10^6 cpm/µl) was annealed with 1 µl of chemically modified ribozyme (1.2 pmol/µl) or control RNA in 6 µl of AB buffer (40 mM TrisHCl, pH 8.3; 4.8 mM NaCl; 8 mM DTT) by boiling for 90 seconds at 90°C and cooling to room temperature. Reverse transcription was performed by adding 6 µl of RT-dNTP mix (40 mM TrisHCl, pH 8.3; 3 units AMV reverse transcriptase; 6 mM $Mg(OAc)_2$; 0.5 mM dNTP) and incubating for 30 min at 25°C. The reaction was stopped by addition of 12 µl of formamide stop buffer and boiled for 3 min before being loaded on a denaturing 20% polyacrylamide gel and analyzed as described above.

Enzymatic probing

The enzymatic digestion reactions were performed in 16 mM sodium citrate buffer (pH 5.5) for RNase U2 and 20 mM Tris-HCl buffer (pH 7.5) for RNase T1, T2, V1, and Nuclease S1 in the presence of 100 mM KCl and 20 mM $MgCl_2$ for 20 min at 30°C. A total of 6 µl of 5′ labeled RNA (2.0×10^6 CPM) solution was incubated with 2 µl of the appropriate diluted RNase solution: 5.0×10^{-3} U/µl of RNase T1, 5.0×10^{-3} U/µl of RNase T2, 10^{02} U/µl of Nuclease S1, 3.6×10^{-5} U/µl of RNase V1 or 1.0 U/µl of RNase U2. The reactions were stopped by adding an equal volume of stop buffer solution (9 M urea, 10% [v/v] glycerol, 0.05% [w/v] XC and 0.05% [w/v] BPB) and by immediately freezing on dry ice. The hydroxide ladder reaction was carried out with 2 µl of 5′ labeled RNA in 4 µl of hydroxide hydrolysis buffer (50 mM $NaHCO_3/Na_2CO_3$, pH 9.2 and 1 mM EDTA) for 5–7 min at 90°C and then immediately plunged into an ice-slurry bath. The control reaction was performed with 2 µl of 5′ labeled RNA in RS buffer (20 mM sodium citrate, pH 5.0, 1 mM EDTA and 7 M urea) for 3 min at 50°C and immediately plunged into an ice-slurry bath. The samples were loaded on a 20% polyacrylamide/7 M urea gel and analyzed as described above.

Mutant ribozymes

Site-specific mutations in the ribozymes were made by first introducing the mutations into the corresponding cDNA templates by PCR amplification using the appropriate primers containing the desired base changes. The PCR was carried out with 0.5 µg of clone 25 plasmid DNA, 2 µM primers, 0.4 mM each dNTP and 5 U Taq DNA polymerase in the presence of 3.0 mM $MgCl_2$ for 25 thermal cycles (94°C for 30s, 55°C for 30s and 72°C for 60s). The products of the PCR mutagenesis were used as templates for runoff transcription reactions, as described above, to generate the desired mutant ribozymes. Ribozyme activity was analyzed as described above.

Acknowledgements

We thank A. Gooding, K. Goodrich and E. Podell for oligonucleotide synthesis, R. Gottlieb and S. Seiwert for comments on the manuscript. B.Z. is supported by a postdoctoral fellowship from the National Institute of General Medical Science, NIH. T.R.C. is an Investigator of the Howard Hughes Medical Institute and an American Cancer Society Professor.

References

1. Cech, T.R. (1993). Structure and mechanism of the large catalytic RNAs: group I and group II introns and ribonuclease P. In *The RNA World.* (Gesteland, R.F. & Atkins, J.F., eds) pp. 239-269, Cold Spring Harbor Laboratory Press, Plainview, NY.
2. Piccirilli, J.A., McConnell, T.S., Zaug, A.J., Noller, H.F. & Cech, T.R. (1992). Aminoacyl esterase activity of the *Tetrahymena* ribozyme. *Science* **256**, 1420-1424.
3. Robertson, D.L. & Joyce, G.F. (1990). Selection *in vitro* of an RNA enzyme that specifically cleaves single-stranded DNA. *Nature* **344**, 467-468.
4. Bartel, D.P. & Szostak, J.W. (1993). Isolation of new ribozymes from a large pool of random sequences. *Science* **261**, 1411-1418.
5. Lorsch, J.R. & Szostak, J.W. (1994). *In vitro* evolution of new ribozymes with polynucleotide kinase activity. *Nature* **371**, 31-36.
6. Prudent, J.R., Uno, T. & Schultz, P.G. (1994). Expanding the scope of RNA catalysis. *Science* **264**, 1924-1927.
7. Dai, X-C, de Mesmaeker, A. & Joyce, G.F. (1995). Cleavage of an amide bond by a ribozyme. *Science* **267**, 237-240.
8. Wilson, C. & Szostak, J.W. (1995). *In vitro* evolution of a self-alkylating ribozyme. *Nature* **374**, 777-782.
9. Ekland, E.H. & Bartel, D.P. (1996). RNA-catalyzed RNA polymerization using nucleoside triphosphates. *Nature* **382**, 373-376.
10. Conn, M.M., Prudent, J.R. & Schultz, P.G. (1996). Porphyrin metalation catalyzed by a small RNA molecule. *J. Am. Chem. Soc.* **118**, 7012-7013.
11. Wecker, M., Smith, D. & Gold, L. (1996). *In vitro* selection of a novel catalytic RNA: characterization of a sulfur alkylation reaction and interaction with a small peptide. *RNA* **2**, 982-994.
12. Tarasow, T.M., Tarasow, S.L. & Eaton, B.E. (1997). RNA-catalyzed carbon–carbon bond formation. *Nature* **389**, 54-57.
13. Illangasekare, M., Sanchez, G., Nickles, T. & Yarus, M. (1995). Aminoacyl-RNA synthesis catalyzed by an RNA. *Science* **267**, 643-647.
14. Lohse, P.A. & Szostak, J.W. (1996). Ribozyme-catalyzed amino-acid transfer reactions. *Nature* **381**, 442-444.
15. Jenne, A. & Famulok, M. (1998). A novel ribozyme with ester transferase activity. *Chem. Biol.* **5**, 23-34.
16. Zhang, B. & Cech, T.R. (1997). Peptide bond formation by *in vitro* selected ribozymes. *Nature* **390**, 96-100.
17. Cech, T., Zaug, A. & Grabowski, P. (1981). *In vitro* splicing of the ribosomal RNA precursor of *Tetrahymena*: involvement of a guanosine nucleotide in the excision of the intervening sequence. *Cell* **27**, 487-496.
18. Guerrier-Takada, C., Gardiner, K., Marsh, T., Pace, N. & Altman, S. (1983). The RNA moiety of ribonuclease P is the catalytic subunit of the enzyme. *Cell*, **35**, 849-857.
19. Joyce, G.F. (1989). RNA evolution and the origins of life. *Nature* **338**, 217-224.
20. Benner, S.A., Ellington, A.D. & Tauer, A.D. (1989). Modern metabolism as a palimpsest of the RNA world. *Proc. Natl Acad. Sci. USA* **86**, 7054-7058.
21. Woese, C.R. (1967). *The Genetic Code: The Molecular Basis for Genetic Expression.* Harper & Row, New York.
22. Crick, F.H.C. (1968). The origin of the genetic code. *J. Mol. Biol.* **38**, 367-379.
23. Ellington, A.D. & Hirao, I. (1995). Re-creating the RNA world. *Curr. Biol.* **5**, 1017-1022.
24. Hager, A., Pollard, J.D. & Szostak, J.W. (1996). Ribozymes: aiming at RNA replication and protein synthesis. *Chem. Biol.* **3**, 717-725.
25. Noller, H.F. (1993). On the origin of the ribosome: coevolution of subdomains of tRNA and rRNA. In *The RNA World.* (Gesteland, R.F. & Atkins, J.F., eds) pp.137-156, Cold Spring Harbor Laboratory Press, Plainview, NY.
26. Noller, H.F., Hoffarth, V. & Zimniak, L. (1992). Unusual resistance of peptidyl-transferase to protein extraction procedures. *Science* **256**, 1416-1419.
27. Zimmermann, R.A. & Dahlberg, A.E. (1996). *Ribosomal RNA: Structure, Evolution, Processing and Function in Protein Biosynthesis.* CRC Press, London.
28. Schofield, P. & Zamecnik, P.C. (1968). Cupric-ion catalysis in hydrolysis of aminoacyl-tRNA. *Biochim. Biophys. Acta* **155**, 410-416.
29. Mathews, D.H., Andre, T.C., Kim, J., Turner, D.H. & Zuker, M. (1998). An updated recursive algorithm for RNA secondary structure prediction with improved free energy parameters. *Am. Chem. Soc. Symp. Ser.* **682**, 246-257.
30. Nitta, I., Ueda, T. & Watanabe, K. (1998). Possible involvement of *Escherichia coli* 23S ribosomal RNA in peptide bond formation. *RNA* **4**, 257-267.
31. Green, R., Switzer, C. & Noller, H.F. (1998). Ribosome-catalyzed peptide-bond formation with A-site substrate covalently linked to 23S ribosomal RNA. *Science* **280**, 286-289.
32. Saarma, U., Spahn, C.M.T., Nierhaus, K.H. & Remme, J. (1998). Mutational analysis of the donor substrate binding site of the ribosomal peptidyl-transferase center. *RNA* **4**, 189-194.
33. Moazed, D. & Noller, H.F. (1989). Interaction of tRNA with 23S rRNA in the ribosomal A, P, and E sites. *Cell* **57**, 585-597.

34. Rodriguez-Fonseca, C., Amils, R. & Garrett, R.A. (1995). Fine structure of the peptidyl-transferase center on 23S rRNAs deduced from chemical probing of antibiotic–ribosome complexes. *J. Mol. Biol.* **247**, 224-235.
35. Hall, C.C., Johnson, D. & Cooperman, B.S. (1988). [^{3}H]-*p*-azidopuromycin photo affinity labeling of *Escherichia coli* ribosomes: evidence for site-specific interaction at U-2504 and G-2502 in domain V of 23S ribosomal RNA. *Biochemistry* **27**, 3983-3990.
36. Moazed, D. & Noller, H.F. (1989). Intermediate states in the movement of transfer RNA in the ribosome. *Nature* **342**, 142-148.
37. Stern, G., Kuechler, E. & Barta, A. (1988). Photo-affinity labeling at the peptidyl-transferase center reveals two different positions for the A- and P-sites in domain V of 23S rRNA. *EMBO J.* **7**, 3949-3955.
38. Symons, R.H., Harris, R.J., Greenwell, P., Eckermann, D.J. & Vanin, E.F. (1978). The use of puromycin analogs and related compounds to probe the active center of peptidyl-transferase on *Escherichia coli* ribosomes. *Bioorg. Chem. (Suppl.)* **4**, 409-436.
39. Moazed, D. & Noller, H.F. (1987). Chloramphenicol, erythromycin, carbomycin and vernamycin B protect overlapping sites in the peptidyl-transferase region of 23S rRNA. *Biochimie* **69**, 879-884.
40. Egebjerg, J. & Garrett, R.A. (1991). Binding sites of the antibiotics pactamycin and celesticetin on rRNAs. *Biochimie* **73**, 1145-1149.
41. Douthwaite, S. (1992). Interaction of the antibiotics clindamycin and lincomycin with *Escherichia coli* 23S rRNA. *Nucleic Acids Res.* **20**, 4717-4720.
42. Porse, B.T., Thi-Ngoc, H.P. & Garrett, R.A. (1996). The donor substrate site within the peptidyl-transferase loop of 23S rRNA and its putative interactions with the CCA-end of N-blocked aminoacyl-tRNA^{Phe}. *J. Mol. Biol.* **264**, 472-483.
43. Welch, M., Majerfeld, I. & Yarus, M. (1997). 23S rRNA similarity from selection for peptidyl-transferase mimicry. *Biochemistry* **36**, 6614-6623.
44. Weiner, A.M. (1993). mRNA splicing and autocatalytic introns: distant cousins or the products of chemical determinism? *Cell* **72**, 161-164.
45. Bass, B.L. & Cech, T.R. (1984). Specific interaction between the self-splicing RNA of *Tetrahymena* and its guanosine substrate: implications for biological catalysis by RNA. *Nature* **308**, 820-826.
46. Herschlag, D. & Cech, T.R. (1990). Catalytic of RNA cleavage by the *Tetrahymena thermophila* ribozyme. 2. Kinetic description of the reaction of an RNA substrate that forms a mismatch at the active site. *Biochemistry* **29**, 10172-10180.
47. Sassanfar, M. & Szostak, J.W. (1993). An RNA motif that binds ATP. *Nature* **364**, 550-553.
48. Gerger, A., Burgstaller, P., von der Eltz, H., Roeder, A. & Famulok, M. (1996). RNA aptamers that bind L-arginine with sub-micromolar dissociation constants and high enantioselectivity. *Nucleic Acids Res.* **24**, 1029-1036.
49. Piccirilli, J.A., Vyle, J.S., Caruthers, M.H. & Cech, T.R. (1993). Metal-ion catalysis in the *Tetrahymena* ribozyme reaction. *Nature* **361**, 85-88.
50. Pyle, A.M. (1993). Ribozymes: a distinct class of metalloenzymes. *Science* **261**, 709-714.
51. Cate, J.H., Hanna, R.L. & Doudna, J.A. (1997). A magnesium ion core at the heart of a ribozyme domain. *Nat. Struct. Biol.* **4**, 553-558.
52. Celander, D.W. & Cech, T.R. (1991). Visualizing the higher order folding of a catalytic RNA molecule. *Science* **251**, 401-407.
53. Dahm, S.C. & Uhlenbeck, O.C. (1991). Role of divalent metal ions in the hammerhead RNA cleavage reaction. *Biochemistry* **30**, 9464-9469.
54. Maden, B.E.H. & Monro, R.E. (1968). Ribosome-catalyzed peptidyl transfer: effects of cations and pH value. *Eur. J. Biochem.* **6**, 309-316.
55. Pace, N.R. (1992). New horizons for RNA catalysis. *Science* **256**, 1402-1403.

Because *Chemistry & Biology* operates a 'Continuous Publication System' for Research Papers, this paper has been published via the internet before being printed. The paper can be accessed from http://biomednet.com/cbiology/cmb – for further information, see the explanation on the contents pages.